Sensors & Actuators: B. Chemical 278 (2019) 140–146

Contents lists available at ScienceDirect

Sensors and Actuators B: Chemical

journal homepage: www.elsevier.com/locate/snb

Development of a self-driving bioassay based on diffusion for simple detection of microorganisms

Jhih-Cheng Wang[a,b], Shao-Wen Chi[a], Dar-Bin Shieh[c], Han-Sheng Chuang[a,d,*]

[a] Department of Biomedical Engineering, National Cheng Kung University, Taiwan
[b] Department of Urology, Cheimei Medical Center, Taiwan
[c] Institute of Oral Medicine, National Cheng Kung University Hospital, Taiwan
[d] Medical Device Innovation Center, National Cheng Kung University, Taiwan

ARTICLE INFO

Keywords:
Diffusion
Microparticles
Bacteria
Brownian motion
Self-driving bioassay

ABSTRACT

A self-driving, thermal-diffusion-based bioassay for the detection of microorganisms in a liquid medium is presented in this paper. In the bioassay, each particle functions as an individual sensing probe. Thus, the representative Brownian velocity of microparticles can be obtained by analyzing the velocity histogram of each particle. The ensemble average was used to enhance peak Brownian velocity. Relative error was reduced to 0.5% when the number of counted particles exceeded 60. The experimentally measured and theoretically derived Brownian velocities and diameters of the particles were in good agreement. The relative standard deviations of the temporal stability and reproducibility of the bioassay were maintained below 1.2%. A calibration curve was constructed and used to distinguish two mixed colloidal suspensions to provide proof that the bioassay can be used in practical applications. The particles were functionalized with antibodies to enable the real biological application of the bioassay in the capture and detection of motile *Pseudomonas aeruginosa* and nonmotile *Staphylococcus aureus*. The diffusivity values of both bacterial growth media decreased as bacterial concentration increased. Given that the viscosity of the growth media varied as bacteria proliferated, additional bacteria-free reference particles were added to the medium to provide dynamic background information. The diffusion-based bioassay presented here is easy to use, robust, and highly reliable. In contrast to most existing biosensors, it does not require an external power source and is thus ideal for use in resource-limited areas.

1. Introduction

Functionalized microparticles have been widely used in the detection of various analytes [1–4]. Although bead-based biosensing methods have high flexibility, sensitivity, and accuracy, their sensitivity, resolution, and reliability are mainly dependent on external readout equipment. The presence of target molecules is indicated by changes in the fluorescence or colors of dye-labeled microparticles [5–7]. Given that light intensity increases with the amount of target molecules, signals of the molecular activities can be quantified with photodetectors or simply interpreted visually. Wang et al. [8] proposed a novel optoelectrokinetic platform that enhances biosignals by concentrating fluorescent microparticles. In this platform, fluorescence is generated through the effect of Förster resonance energy transfer. The platform achieves a limit of detection of as low as 5 nM for the target protein lipocalin 1. In recent years, label-free methods have received considerable attention from the public because they enable the highly reliable quantification of target analytes. Kinnunen et al. [9] reported a novel method for determining the drug susceptibility of bacteria. Their reported method is based on an asynchronous magnetic particle rotation sensor driven by external electromagnetic coils. The magnetic particles were coated with vancomycin to capture free motile *Escherichia coli* cells. In this sensing system, particle rotation is altered by the surface attachment of bacteria. The alteration in particle rotation is terminated under the effect of antibiotic. In contrast to conventional antimicrobial susceptibility testing (AST), their method can determine the drug susceptibility of bacteria within 2 h. Zhao et al. [10] later developed a paper-based bioassay using DNA-modified gold nanoparticles deposited on paper substrates. The color of the paper substrate changes from blue to red when the dispersed gold nanoparticles aggregate in the presence of DNase I or adenosine. Qian et al. [11] attempted in vivo tumor targeting and detection by using surface-enhanced Raman (SERS) nanoparticle tags, which offer enhanced sensitivity, multiplexing, and quantification. The SERS nanoparticle

* Corresponding author at: Department of Biomedical Engineering, National Cheng Kung University, Taiwan.
E-mail address: oswaldchuang@mail.ncku.edu.tw (H.-S. Chuang).

https://doi.org/10.1016/j.snb.2018.09.087
Received 12 June 2018; Received in revised form 19 September 2018; Accepted 21 September 2018
Available online 26 September 2018

tags have been used successfully in the spectroscopic detection of small tumors (0.03 cm^3) with the penetration depth of 1–2 cm. Despite their advantages, however, the above methods require costly and sophisticated instruments for signal extraction. To eliminate the dependence of detection methods on external equipment, Gorti et al. [12] proposed bead-based diffusometry for viral detection. In this method, the diffusive state of microparticles in a medium could be monitored by measuring the width of a correlation peak obtained from the images of randomly moving particles. Diffusometric detection methods are failure-free because they rely solely on the self-driven Brownian motion of microparticles.

Diffusometric bioassays are more practical and suitable for real clinical applications than existing bioassays [13–18] because they do not depend on external power supplies and light intensity for detection. We have previously proven the feasibility of bead-based diffusometry for rapid AST [19,20], diabetic retinopathy diagnosis [21], and viscosity measurements [22,23]. In contrast to previous researchers who applied cross-correlation functions to characterize their diffusometric techniques, we characterized our technique by using the probability distribution function (PDF) of Brownian velocity measured over the duration of 33 s. Moreover, we evaluated the performance of our method on the basis of several parameters, including the number of images and data points, as well as magnification and stability. Notably, all microparticles were tracked individually in consecutive images. Then, we obtained the peak Brownian velocity to represent the diffusive state of all microparticles. Collective particle behaviors can be represented by statistical parameters because each microparticle functions as a self-driven biosensing probe. The results of our evaluations suggested that at least 80 data points are required to construct a meaningful velocity histogram, and the ensemble average of more than 60 particles is needed to obtain distinct Brownian velocities. The measured and predicted peak Brownian velocities of particles with different diameters were in good agreement. Temporal stability and reproducibility showed relative errors of less than 1%. Large and small particle sizes, however, resulted in parallel shifts away from predicted values because of the poor identification of particle displacement. We then successfully applied our approach in the identification of two colloidal suspensions containing particles with different sizes. Finally, we functionalized microparticles with antibodies to capture *Pseudomonas aeruginosa* and *Staphylococcus aureus*. Both bacterial species could be detected using our bioassay in a dose-dependent manner. Notably, motile microorganisms may increase Brownian velocities by boosting microparticle diffusion. Nonetheless, diffusivity tended to decline with bacterial concentration. We counteracted background noise through the addition of reference microparticles to the same buffer medium. Our diffusion-based self-driving bioassay can provide a cornerstone for the rapid screening of other pathogenic microorganisms.

2. Methods and materials

2.1. Measurement system

The diffusometric platform comprised a fluorescent microscope (IX71, Olympus), a digital CMOS camera (FL3-U3-13S2C-CS, Point Grey Research Inc.), a computer, and a glass chip (Fig. 1A). The glass chip was simply constructed using a glass slide and a cover glass separated by a spacer (110 μm). A drop of analyte (5 μL) was pipetted on the glass chip for measurement. The microscope was equipped with a filter cube (U-MWIB3, BP460-495/BM505/BA510-IF, Olympus) and objectives with different powers (10×, 20×, and 40×) in accordance with the fluorescent microparticles used. The measurement plane was focused on the central depth of the glass chip to avoid impeding diffusion. To acquire images with good quality, the digital camera was set at a frame rate of 15 Hz in color mode. A total of 500 image frames were recorded for the duration of 33 s for each measurement. Although the system did not need to be set up on a vibration-free table, interferences from nearby fans or experiments on the same table were avoided. The laboratory temperature was controlled at 24 °C with an air conditioner. Slight variations in medium temperature and viscosity can be cancelled out through the addition of reference microparticles. In the absence of reference microparticles, however, the relative error due to the temperature variation of ± 1 °C was estimated to be less than 0.6%.

2.2. Diffusion-based algorithm

The Stokes–Einstein relation [24] states that diffusivity is inversely proportional to particle diameter when all other parameters are controlled. Langevin's theory is used to describe the relationship between time-averaged Brownian velocity and diffusivity [25]. Each functionalized microparticle can be used as a biosensing probe by simply tracking its Brownian velocity over time (Fig. 1B). The Brownian velocities of numerous particles are needed to construct a histogram that provides meaningful information. Data points were fitted with a six-order polynomial curve, and peak velocity was derived from the first-order derivatives of the curve. Through ensemble average with numerous velocity histograms, the diffusion-based algorithm was stabilized, and the effects of background fluctuations were avoided. The velocity histogram was created by sorting Brownian velocities within the measurement duration (500 frames at 15 Hz). All individual particles were tracked by using the ImageJ (https://fiji.sc/) plug-in program PTA2 (https://github.com/arayoshipta/PTA2). Image processing is described in detail in the Supplementary Information section. The maximum point of the polynomial curve was taken as the representative Brownian velocity for the diffusive state of a selected particle. In principle, the peak Brownian velocity of a small particle is larger than that of a large particle. Given that Brownian velocity is sensitive to the change in the size of each microparticle, in this study, microparticles were functionalized with antibodies to capture specific microorganisms. Although particle shape may alter Brownian velocity, variations among microparticles can be averaged out through the addition of reference microparticles.

The viscosity and temperature of a complicated medium, such as biological buffers, may slightly vary with time because of inhomogeneity in contents. To alleviate variations, reference particles were added to the same medium to provide information on background fluctuations. Thus, the relative Brownian velocity of a single microparticle can be expressed as

$$\frac{S}{S_0} = \frac{\sqrt{d_{p0}}}{\sqrt{d_p}} \tag{1}$$

where d_{p0} and d_p represent the diameters of the reference and probe particles, respectively. The relative Brownian velocity is only associated with the change in particle size and is unaffected by other disturbances, i.e., changes in viscosity and temperature.

2.3. Reagents and microorganisms

Bovine serum albumin (BSA), 1-ethyl-3-(3-dimethylaminopropyl) carbodiimide (N), N-hydroxysuccinimide (NHS), 2-(n-morpholino)-ethanesulfonic acid (MES), and gentamicin were obtained from Sigma-Aldrich (St. Louis, MO, USA). Anti-*P. aeruginosa* polyclonal antibody (Ab, ab67905), anti-*S. aureus* polyclonal Ab (ab20920), and anti-TNF-α monoclonal Ab (ab9348) were acquired from Abcam (Cambridge, MA, USA). Tryptic soy broth (TSB) was obtained from BD (East Rutherford, NJ, USA).

2.4. Microparticle functionalization

Four plain fluorescent polystyrene (PS) particles with sizes of 0.5, 1, 3.2, and 4.8 μm (G500/R0100/R0300/G0500, 1% solids, Thermo

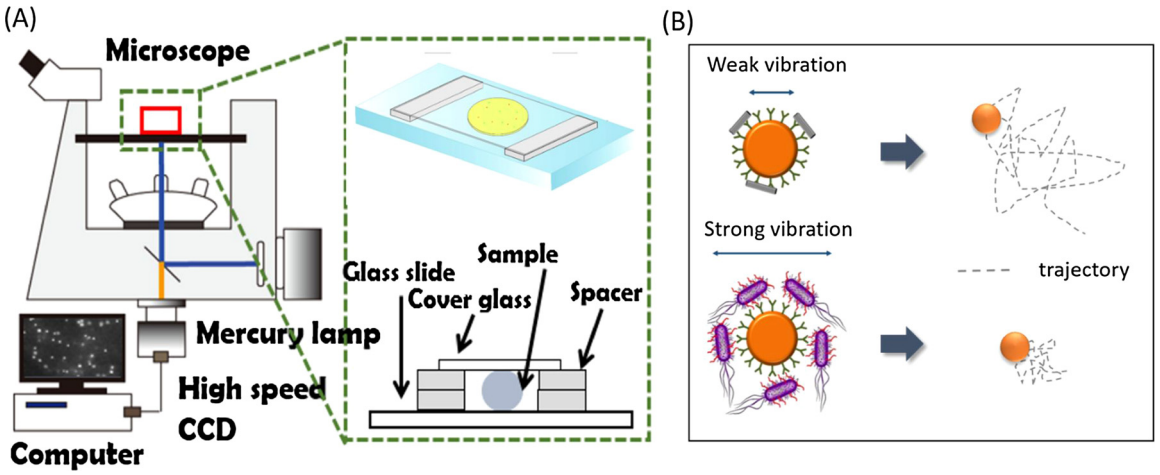

Fig. 1. (A) Schematic of the measurement system including a close-up of the glass chip configuration. (B) Concept of biosensing probes for microorganisms based on Brownian motion.

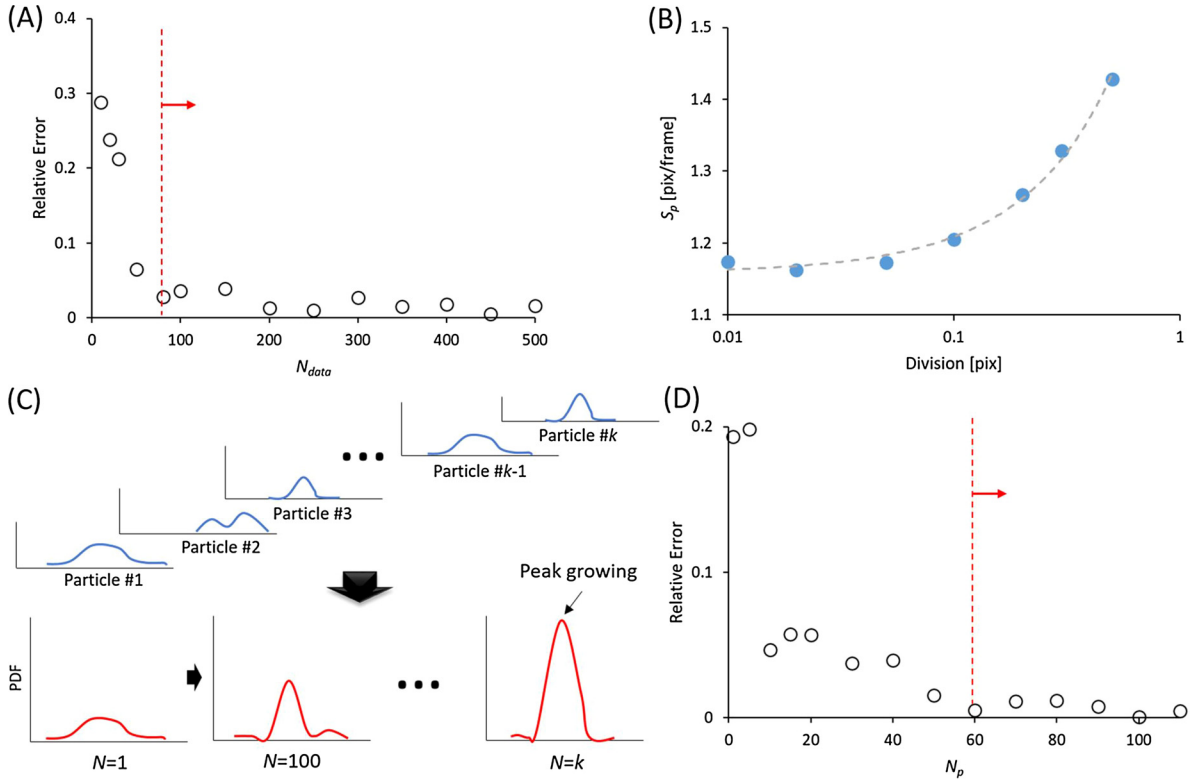

Fig. 2. (A) Effect of the number of data points on relative error. The red dotted line indicates a turning point at N_{data} = 80. (B) Variation in peak Brownian velocity with different divisions of group sorting. (C) Conceptual illustration of the ensemble average of the velocity histograms of microparticles. (D) Effect of the ensemble average of the velocity histograms of microparticles on relative error. The red dotted line indicates a relative error of less than 0.5% at N_p = 60. (For interpretation of the references to colour in this figure legend, the reader is referred to the web version of this article.)

Fisher Scientific) and carboxylate-modified PS particles (L4530, 2.5% solids, Sigma Aldrich) with sizes of 2 μm were used for the initial calibration in the evaluation of the proposed diffusometric system. The size uniformities of the PS and carboxylate-modified PS particles were less than 5% and 10% CV, respectively. Yellow-green carboxylate-modified PS particles (L4530, Ex/Em: 470/505, Sigma Aldrich) and red (L9529, Ex/Em: 520/540, Sigma Aldrich) amine-modified PS particles with sizes of 2 μm were used as functionalized microparticles. To conjugate amine-modified PS particles with antibodies, 2 μL of microparticles (2% volumetric ratio) were first washed five times with phosphate-buffered saline with Tween-20 (PBST). Next, 43 μL of 10 μg/μL NHS, 2 μL of 10 mg/mL EDC, and 34 μL of 50 mM MES (pH = 5.5) were mixed with the antibodies for carboxyl group activation and incubated for 15 min in a shaker at 25 °C. The activated antibodies were then mixed with the particle suspension in PBST with MES in a shaker for 4 h at 4 °C. Excess antibodies were removed with PBST through centrifugation at 9500 rpm for five cycles. Then, to block nonspecific binding, 1% BSA (A2153, Sigma) and the suspension were mixed for 1 h in a shaker at 25 °C. Finally, the solution was washed thrice with PBST and centrifugation at 9500 rpm. The total volume of the solution was maintained at 200 μL for each wash cycle. After washing, the functionalized microparticles were ready to be used for the detection of bacteria suspended in a sample medium. Specific bacteria and functionalized microparticles were mixed in a shaker for 2 h at 25 °C before

measurement.

2.5. Bacterial culture

P. aeruginosa (ATCC 27853), a motile Gram-negative rod (0.5–1 × 1.5–3 μm) bacterial species, and *S. aureus* (ATCC 23360), a nonmotile Gram-positive coccus (1–2 × 1–2 μm) bacterial species were gifted by Dr. H. C. Chang's laboratory, Department of Biomedical Engineering, National Cheng Kung University. *P. aeruginosa* and *S. aureus* were incubated in TSB with shaking for 12–16 h at 37 °C before use.

3. Results and discussion

3.1. Evaluation of the diffusion-based algorithm

The relative errors of the diffusion-based algorithm were evaluated on the basis of the number of data points and the number of microparticles. In the evaluations, Brownian velocities of 1-μm particles were measured under 20× magnification. The relative error for each single microparticle with respect to the number of valid data points decreased to less than 3% when the data excess $N_{data} = 80$ (Fig. 2A) given that the number of data points was insufficient for constructing a meaningful histogram. To avoid serious deviations, microparticles were considered only when their data points exceeded 200. In addition, division size influenced the resolution of the velocity histogram. The relationship between peak Brownian velocity and division size is depicted in Fig. 2B. The peak Brownian velocity stabilized when the division size fell between 0.05 pixels. A small division size, however, required additional data points to form a well-distributed histogram. The acceptable division size was then determined as 0.1 under the current condition.

Given that the microparticles were uniform in size and the medium was homogeneous, true Brownian velocity emerged when the total numbers of the velocity histograms of particles increased (Fig. 2C). The ensemble average has good ability to represent true values without disturbance by extreme outliers [26]. The velocity histograms of 1 μm microparticles with 200 data points were constructed. Relative error decreased to less than 5% after the addition of five peak velocities and further decreased to 0.5% after the number of microparticles increased to $N_p = 60$ (Fig. 2D). Given this information, the subsequent constructions of velocity histograms, unless mentioned otherwise, required at least 60 microparticles for the determination of peak Brownian velocities.

3.2. Peak Brownian velocities with respect to particle sizes

To establish a database that includes the peak Brownian velocities of particles with different sizes (nominal size: $d_p = 0.5$, 1, 2, 3, and 5 μm), fluorescent images of the particles were recorded at a frame rate of 15 Hz under 20× and 40× magnification for 33.3 s. The ensemble average of the velocity histograms of more than 60 microparticles was obtained, and only histograms containing 200 data points were selected. The velocity histograms and final peak Brownian velocities of all microparticles are depicted in Fig. 3A–E. The representative Brownian velocities of microparticles with sizes of 0.5, 1, 2, 3, and 5 μm under 20× magnification were 1.65, 1.21, 0.88, 0.76, and 0.59 pixel/frame, respectively. By dividing the peak velocities (S) by the maximum velocity (S_0), the relationship of normalized peak velocity and particle size was determined and is illustrated in Fig. 3F. Similar to particles with other sizes, the 2-μm particles were fabricated from PS. Given that diffusivity is only subject to volume change on the microscale, the thin layer of functional groups on the 2-μm particles is therefore negligible, and the trend of relative Brownian velocity versus microparticle diameter is independent of magnification. The experimental data show good agreement with the theoretical curve constructed using the equation $\langle S \rangle = \sqrt{2Dt}$. This result implies the correctness and accuracy of the diffusion-based technique.

3.3. Effect of magnification

Magnification may affect the accuracy of experimental measurements because Brownian velocity is calculated by using particle images. To understand the effect of magnification, particles with sizes of 1, 2, or 5 μm were investigated under the nominal magnifications of 10×, 20×, and 40× (Fig. 4A–C). The estimated magnifications were experimentally determined as 10.01×, 19.97×, and 39.13× (refer to the Supplementary Information for the experimental procedure). All three particle sizes show distinct peak Brownian velocities under different magnifications. Experimental data were compared with theoretical predictions, and the relationships between experimental data and theoretical predictions are depicted in Fig. 4D. In general, the correlation factors for all three cases exceeded 95%. High magnification resolved more detailed changes in Brownian velocity than low magnification but suffered from low data rates and high out-of-focus loss-of-pairs. By contrast, low magnification featured high data rates and low out-of-focus loss-of-pairs. As a result, in contrast to that of its counterparts, the experimentally measured peak Brownian velocity of 5 μm particles deviated from the predicted value, particularly when measured under 40× magnification. Nonetheless, the experimentally measured peak Brownian velocities remained coincident with theoretical predictions and are linearly proportional to magnification.

3.4. Identification of particles with different sizes in mixed colloidal suspensions

The established database was used in the investigation of two mixed colloidal suspensions. Microparticles possessing at least 200 data points were randomly selected from images for size identification. The value of peak Brownian velocity was checked with the theoretical curve shown in Fig. 3F for the derivation of the corresponding particle size. To prepare the first mixed suspension, 2 μL of 2 μm particles and 6 μL of 3.2 μm particles were simultaneously resuspended in 400 μL of deionized (DI) water (Fig. 5A). The identification results show two distinct groups of particle sizes with one centered at 2 μm and the other at 3 μm (Fig. 5B). To prepare the second mixed suspension, 1 μL of 0.5 μm particles, 2 μL of 1 μm particles, and 4 μL of 2 μm particles were simultaneously resuspended in 400 μL of DI water (Fig. 5C). Similar to the results for the first suspension, those for the second suspension showed three distinct groups of particle sizes centered at 0.68, 1.02, and 1.87 μm (Fig. 5D). The broad histogram and the unknown fourth peak were mainly attributed to fluctuations in peak locations resulting from image defects and variations in microparticle size resulting from manufacturing. As the number of measured microparticles increased, the measured particle sizes tended to approximate nominal sizes, and noise peaks were mitigated. Although noise peaks may not be completely removed during processing, uncertainty can be reduced by setting a threshold of 0.5.

3.5. Detection of live bacteria

Microparticles were functionalized with antibiotics and used as probes to detect the presence of *P. aeruginosa* and *S. aureus*. *P. aeruginosa* is a representative Gram-negative and motile bacterial species, whereas *S. aureus* is a representative Gram-positive and nonmotile bacterial species. The bacteria were initially mixed with antibody-functionalized microparticles (red) and incubated for 2 h in a shaker at 37 °C. Both the bacterial cultures were separately measured when they reached the concentrations of 10^6 and 10^8 cfu/mL after incubation (Fig. 6A). To prevent background disturbances, anti-TNF-α IgG conjugated microparticles (yellow green) were added to the suspension as references (Fig. 6B). According to Eq. (1), the relative Brownian velocity S/S_0 represents only the size change of the probe microparticles.

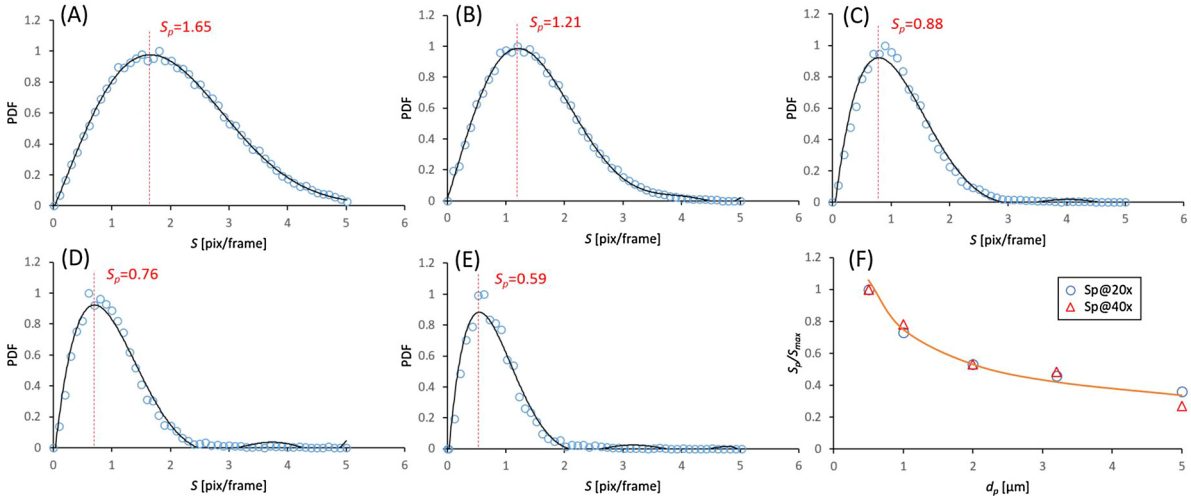

Fig. 3. Brownian velocity histograms of particles with sizes of (A) 0.5, (B) 1, (C) 2, (D) 3, and (E) 5 μm viewed under 20× magnification. (F) Comparison between the experimental data acquired under 20× and 40× magnification and the theoretical curve.

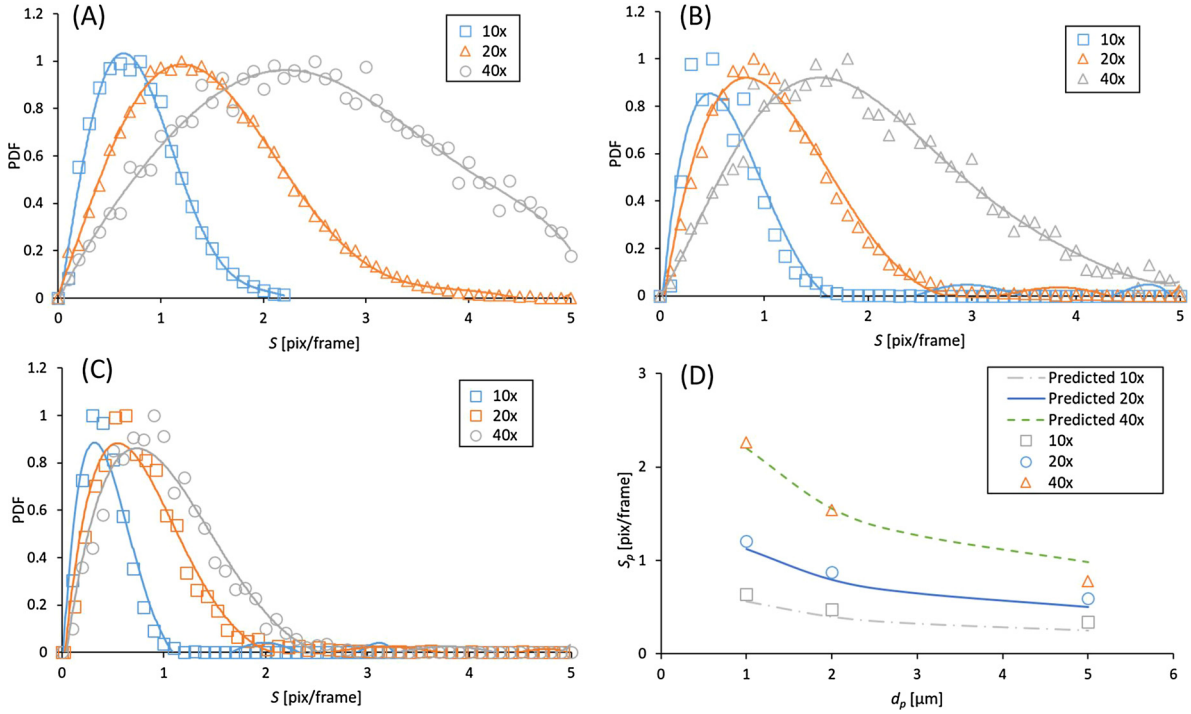

Fig. 4. Evaluations of different particle sizes measured under 10×, 20×, and 40× magnifications. Brownian velocity histograms of particles with sizes of (A) 1, (B) 2, and (C) 5 μm. (D) Comparisons between the peak Brownian velocities of particles with different sizes measured under different magnifications and their theoretical curves.

Therefore, in theory, relative Brownian velocity will be altered only when bacteria attach to the microparticles. Relative Brownian velocity declined in the presence of *P. aeruginosa* and *S. aureus* in a dose-dependent manner (Fig. 6C). Higher Brownian velocities are obtained in the presence of *P. aeruginosa* than *S. aureus* at both concentrations mainly because of the motility of the former.

4. Conclusions

We developed a bead-based bioassay that is driven by Brownian motion. The Stokes–Einstein relation states that particle size is correlated with Brownian velocity when temperature and liquid viscosity are constant. Functionalized microparticles conjugated with the appropriate ligands can serve as sensing probes in a biological medium. Measurement errors were alleviated when the data points of each microparticle exceeded 80 and the velocity histograms of at least 60 microparticles were added. The experimentally measured and theoretically predicted peak Brownian velocities of microparticles with sizes of 0.5 μm–5 μm showed good agreement. In addition, Brownian velocity was linearly proportional to magnification. The system achieved high temporal stability and reproducibility. Two mixed colloidal suspensions were successfully identified using the proposed technique. The functionalized microparticles were also used to detect the presence of *P. aeruginosa* and *S. aureus*. The change in peak Brownian velocity was dependent on bacterial concentration. Results suggest that our proposed self-driving bioassay can be used to detect target analytes in resource-limited areas.

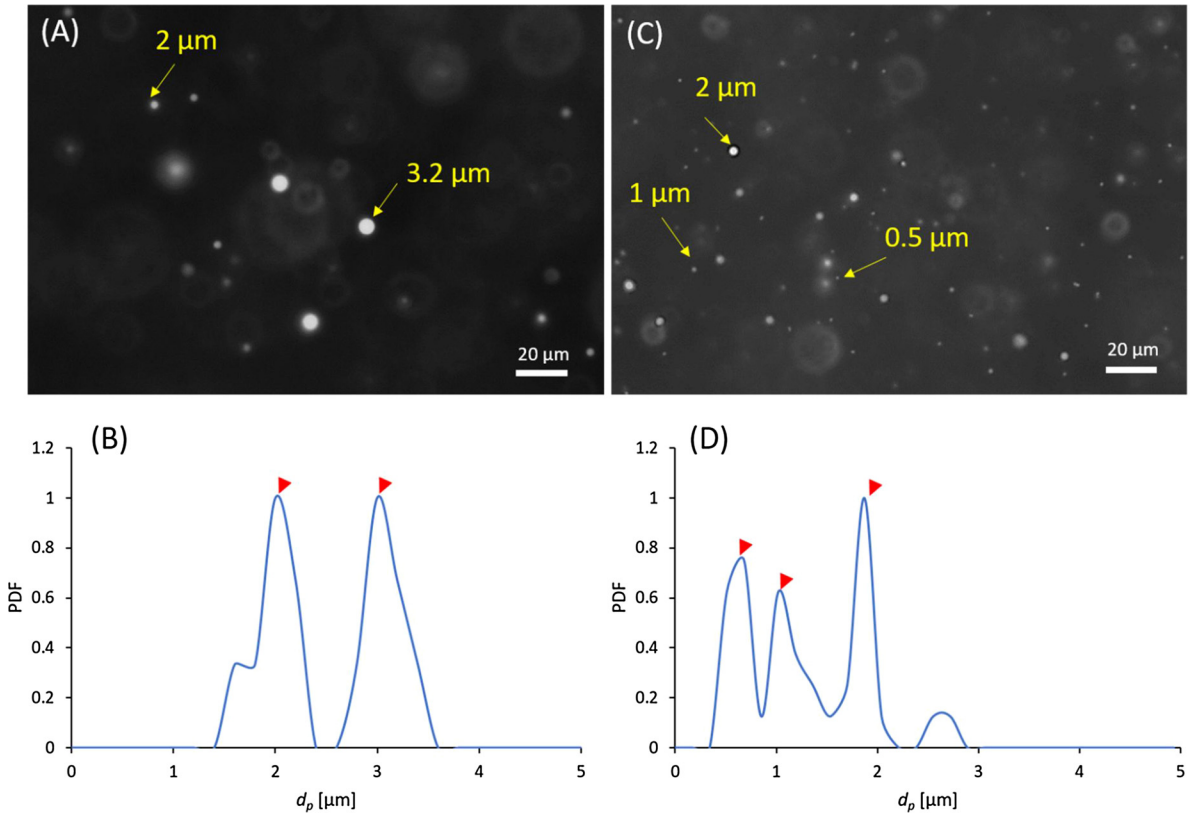

Fig. 5. (A) Image of a colloidal suspension containing microparticles with sizes of 2 and 3.2 μm (representative microparticles are marked by arrows). (B) Size identification results for the suspension containing microparticles with sizes of 2 and 3.2 μm. The two peaks indicated by the red arrows represent particle sizes of 2 (left) and 3 μm (right). (C) Image of a colloidal suspension containing microparticles with sizes of 0.5, 1, and 2 μm (representative microparticles are marked by arrows). (D) Size identification results for the suspension containing microparticles with sizes of 0.5, 1, and 2 μm. The three peaks indicated by red arrows represent particle sizes of 0.68 (left), 1.02 (middle) and 1.87 μm (right). (For interpretation of the references to colour in this figure legend, the reader is referred to the web version of this article.)

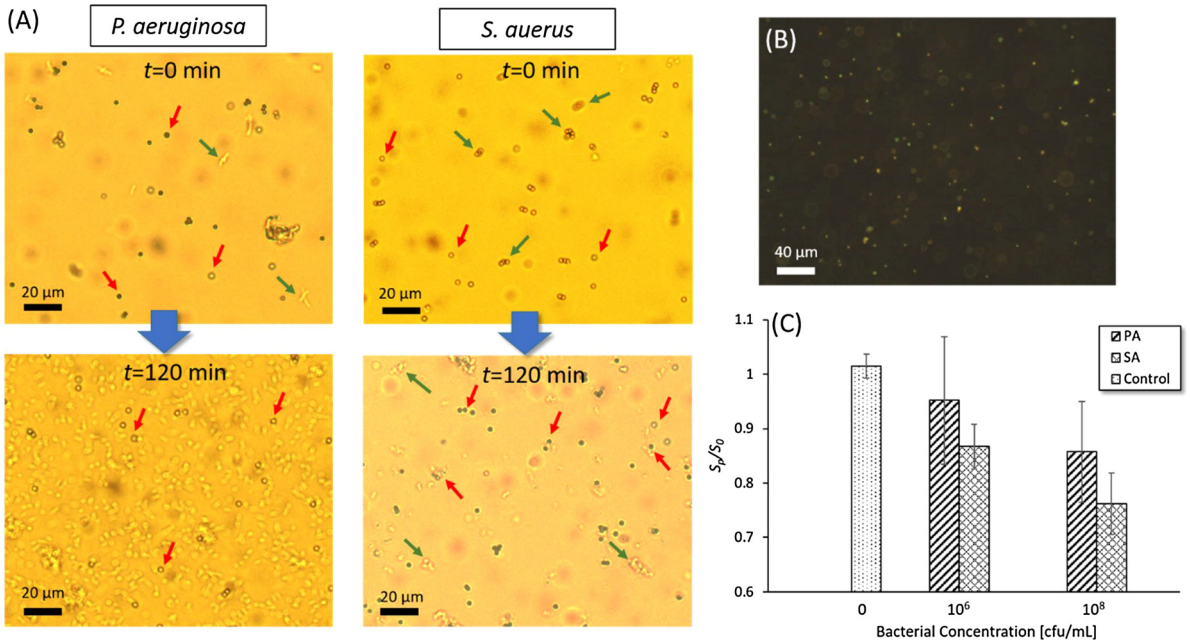

Fig. 6. (A) Images showing bacterial growth in mixed colloidal suspensions (P. aeruginosa and S. aureus) after 120 min of incubation. Red arrows indicate microparticles, and green arrows indicate bacteria. (B) Actual color image taken in fluorescent mode. Microparticles functionalized with antibodies to capture bacteria are shown in red. Microparticles coated with irrelevant antibodies to prevent nonspecific binding and serve as background references are shown in green. (C) Relative Brownian velocities in the presence of two bacterial species with concentrations of 10^6 and 10^8 cfu/mL. The motile P. aeruginosa imparts higher diffusivity to microparticles than its nonmotile counterpart. (For interpretation of the references to colour in this figure legend, the reader is referred to the web version of this article.)

Acknowledgments

The authors are grateful to the Ministry of Science and Technology for the financial support under the grant number 106-2221-E-006-009-CC1 and the grant CMNCKU10612 from Chimei Medical Center.

Appendix A. Supplementary data

Supplementary material related to this article can be found, in the online version, at doi:https://doi.org/10.1016/j.snb.2018.09.087.

References

[1] J.V. Jokerst, Z. Chen, L. Xu, R. Nolley, E. Chang, B. Mitchell, J.D. Brooks, S.S. Gambhir, A magnetic bead-based sensor for the quantification of multiple prostate cancer biomarkers, PLoS One 10 (2015) e0139484.
[2] S.H. Lee, H.-W. Rhee, D. van Noort, H.J. Lee, H.H. Park, I.-S. Shin, J.-I. Hong, T.H. Park, Microfluidic bead-based sensing platform for monitoring kinase activity, Biosens. Bioelectron. 57 (2014) 1–9.
[3] R. Riahi, S.A.M. Shaegh, M. Ghaderi, Y.S. Zhang, S.R. Shin, J. Aleman, S. Massa, D. Kim, M.R. Dokmeci, A. Khademhosseini, Automated microfluidic platform of bead-based electrochemical immunosensor integrated with bioreactor for continual monitoring of cell secreted biomarkers, Sci. Rep. 6 (2016) 24598.
[4] J. Lee, K. Icoz, A. Roberts, A.D. Ellington, C.A. Savran, Diffractometric detection of proteins using microbead-based rolling circle amplification, Anal. Chem. 82 (2010) 197–202.
[5] K. Nishi, S.-I. Isobe, Y. Zhu, R. Kiyama, Fluorescence-based bioassays for the detection and evaluation of food materials, Sensors 15 (2015) 25831–25867.
[6] Y. Kwang-Seok, L. Dohoon, K. Hak-Sung, Y. Euisik, A microfluidic chip for measurement of biomolecules using a microbead-based quantum dot fluorescence assay, Meas. Sci. Technol. 17 (2006) 3178–3183.
[7] K.-C. Wang, A. Kumar, S.J. Williams, N.G. Green, K.C. Kim, H.-S. Chuang, An optoelectrokinetic technique for programmable particle manipulation and bead-based biosignal enhancement, Lab Chip 14 (2014) 3958–3967.
[8] J.-C. Wang, H.-Y. Ku, D.-B. Shieh, H.-S. Chuang, A bead-based fluorescence immunosensing technique enabled by the integration of Förster resonance energy transfer and optoelectrokinetic concentration, Biomicrofluidics 10 (2016) 014113.
[9] P. Kinnunen, I. Sinn, B.H. McNaughton, D.W. Newton, M.A. Burns, R. Kopelman, Monitoring the growth of individual bacteria using asynchronous magnetic bead rotation sensors, Biosens. Bioelectron. 26 (2011) 2751–2755.
[10] W. Zhao, M.M. Ali, S.D. Aguirre, M.A. Brook, Y. Li, Paper-based bioassays using gold nanoparticle colorimetric probes, Anal. Chem. 80 (2008) 8431–8437.
[11] X. Qian, X.-H. Peng, D.O. Ansari, Q. Yin-Goen, G.Z. Chen, D.M. Shin, L. Yang, A.N. Young, M.D. Wang, S. Nie, In vivo tumor targeting and spectroscopic detection with surface-enhanced Raman nanoparticle tags, Nat. Biotechnol. 26 (2007) 83–90.
[12] V.M. Gorti, H. Shang, S.T. Wereley, G.U. Lee, Immunoassays in nanoliter volume reactors using fluorescent particle diffusometry, Langmuir 24 (2008) 2947–2952.
[13] J. Lee, J. Jang, B. Choi, J. Yoon, J.-Y. Kim, Y.-K. Choi, D. Myong Kim, D. Hwan Kim, S.-J. Choi, A highly responsive silicon nanowire/amplifier MOSFET hybrid biosensor, Sci. Rep. 5 (2015) 12286.
[14] A. Poghossian, M.J. Schöning, Label-free sensing of biomolecules with field-effect devices for clinical applications, Electroanalysis 26 (2014) 1197–1213.
[15] L. Malic, K. Morton, L. Clime, T. Veres, All-thermoplastic nanoplasmonic microfluidic device for transmission SPR biosensing, Lab Chip 13 (2013) 798–810.
[16] H.T. Ngo, H.-N. Wang, A.M. Fales, T. Vo-Dinh, Plasmonic SERS biosensing nanochips for DNA detection, Anal. Bioanal. Chem. 408 (2016) 1773–1781.
[17] S.P. Singh, S. Kang, J.W. Kang, P.T.C. So, R.R. Dasari, Z. Yaqoob, I. Barman, Label-free characterization of ultra violet-radiation-induced changes in skin fibroblasts with Raman spectroscopy and quantitative phase microscopy, Sci. Rep. 7 (2017) 10829.
[18] T. Bertok, A. Sediva, J. Katrlik, P. Gemeiner, M. Mikula, M. Nosko, J. Tkac, Label-free detection of glycoproteins by the lectin biosensor down to attomolar level using gold nanoparticles, Talanta 108 (2013) 11–18.
[19] C.-Y. Chung, J.-C. Wang, H.-S. Chuang, Simultaneous and quantitative monitoring of co-cultured Pseudomonas aeruginosa and Staphylococcus aureus with antibiotics on a diffusometric platform, Sci. Rep. 7 (2017) 46336.
[20] C.-Y. Chung, J.-C. Wang, H.-S. Chuang, Rapid bead-based antimicrobial susceptibility testing by optical diffusometry, PLoS One 11 (2016) e0148864.
[21] H.-S. Chuang, Y.-J. Chen, H.-P. Cheng, Enhanced diffusometric immunosensing with grafted gold nanoparticles for detection of diabetic retinopathy biomarker tumor necrosis factor-α, Biosens. Bioelectron. 101 (2018) 75–83.
[22] Y.-S. Sie, H.-S. Chuang, A micro-volume viscosity measurement technique based on μPIV diffusometry, Microfluid. Nanofluid. 16 (2014) 65–72.
[23] W.-J. Kuo, Y.-S. Sie, H.-S. Chuang, Characterizations of kinetic power and propulsion of the nematode *Caenorhabditis elegans* based on a micro-particle image velocimetry system, Biomicrofluidics 8 (2014) 024116.
[24] A. Einstein, R. Fürth, Investigations on the Theory of Brownian Movement, Dover Publications, New York, N.Y, 1956.
[25] P. Langevin, Sur la théorie du mouvement brownien, CR Acad. Sci. Paris 146 (1908) 530–533.
[26] C.D. Meinhart, S.T. Wereley, J.G. Santiago, A PIV algorithm for estimating time-averaged velocity fields, J. Fluids Eng. 122 (2000) 285–289.

Jhih-Cheng Wang received his PhD degree from the Department of Biomedical Engineering at National Cheng Kung University, Taiwan. He is currently a medical doctor in the Department of Urology at Chimei Medical Center, Tainan, Taiwan.

Shao-Wen Chi is a graduate student in the Department of Biomedical Engineering at National Cheng Kung University, Tainan, Taiwan.

Dar-Bin Shieh is currently a professor in the Institute of Oral Medicine at National Cheng Kung University Hospital, Tainan, Taiwan. His research interests focus on nanobiotechnology, oral diagnosis and pathology, molecular biology, cancer biology.

Han-Sheng Chuang is currently an associate professor in the Department of Biomedical Engineering at National Cheng Kung University, Taiwan. His research interests focus on biomicrofluidics, MEMS/NEMS technology, optical diagnostics, and biomechanics of microorganisms.